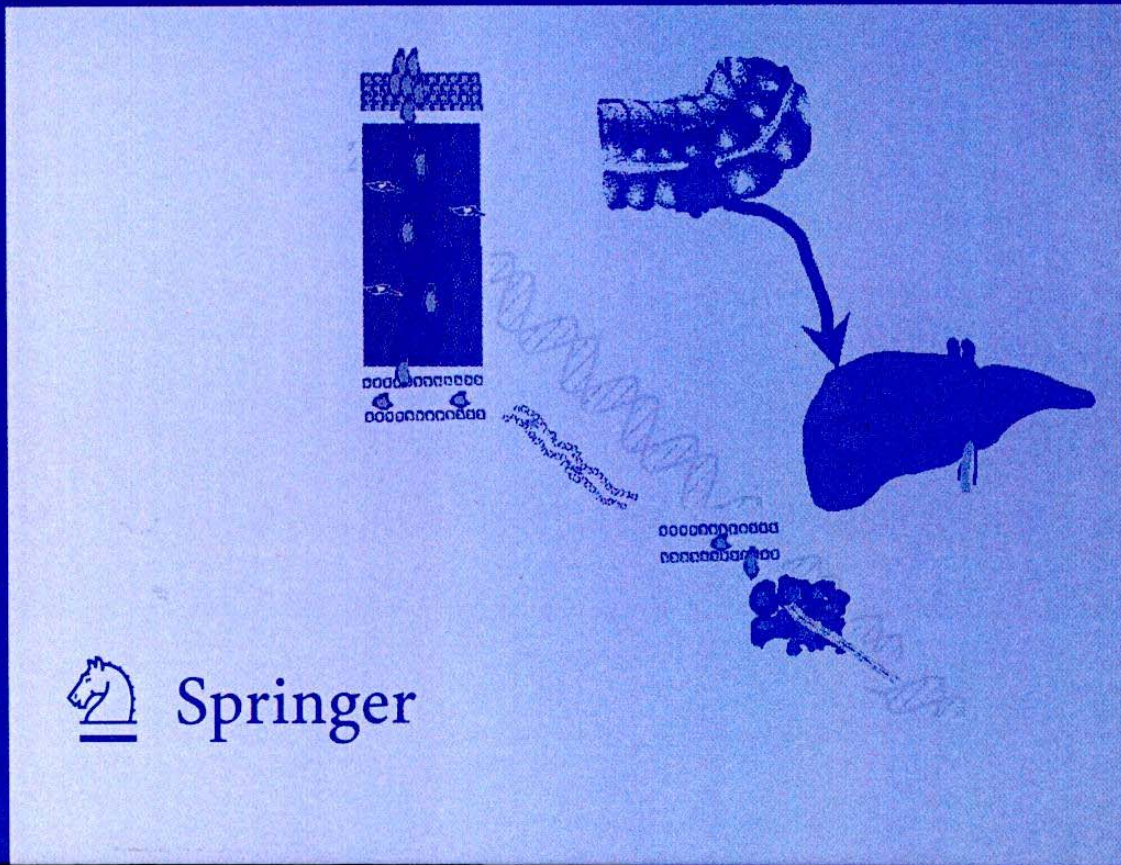


Richard J. Ablin
Malcolm D. Mason
Editors

Cancer Metastasis - Biology and Treatment 10

Metastasis of Prostate Cancer




 Springer

TABLE OF CONTENTS

List of Contributors	ix
Chapter 1	1
Introduction: Metastasis as a Therapeutic Target Richard J. Ablin and Malcolm D. Mason	
Chapter 2	5
The Natural History of Prostate Cancer David F. Penson and Peter C. Albertsen	
Chapter 3	21
The Search for Genes Which Influence Prostate Cancer Metastasis: A Moving Target? Norman J. Maitland	
Chapter 4	63
Polyunsaturated Fatty Acids and Prostate Cancer Metastasis Wen G. Jiang	
Chapter 5	87
Role of Prostaglandin Synthesis and Cyclooxygenase-2 in Prostate Cancer and Metastasis Alaa F. Badawi	
Chapter 6	111
Cell Cycle Regulation Ruchi M. Newman and Bruce R. Zetter	

Chapter 7	127
Epithelial-Mesenchymal Molecular Interactions in Prostatic Tumor Cell Plasticity	
Mary J.C. Hendrix, Jun Luo, Elisabeth A. Seftor, Navesh Sharma, Paul M. Heidger Jr., Michael B. Cohen, Robert Bhattya, Jirapat Chungthapong, Richard E.B. Seftor, and David Lubaroff	
Chapter 8	143
Orthotopic Metastatic Mouse Models of Prostate Cancer	
Robert M. Hoffman	
Chapter 9	171
β-Catenin, its Binding Partners and Signalling Mechanisms: Implications in Prostate Cancer	
Gaynor Davies, Gregory M. Harrison, and Malcolm D. Mason	
Chapter 10	197
Hepatocyte Growth Factor/Scatter Factor and Prostate Cancer Metastasis	
Gaynor Davies, Wen G. Jiang, and Malcolm D. Mason	
Chapter 11	221
Matrix Degradation in Prostate Cancer	
Michael J. Wilson and Akhouri A. Sinha	
Chapter 12	253
The Biology of Bone Metastases from Prostate Cancer and the Role of Bisphosphonates	
Noel W. Clarke and Herbert A. Fleisch	
Chapter 13	283
Non-Steroidal Anti-Androgen Use as Part of Combined Androgen Blockade Therapy for Metastatic or Locally Advanced Prostate Cancer: A Review of the Evidence on Efficacy and Toxicity	
Mike Shelley, Charles Bennett, Derek Nathan, and Oliver Sartor	
Chapter 14	309
Strategies for the Implementation of Chemotherapy and Radiotherapy	
Paula Scullin, Joe M. O'Sullivan, and Christopher C. Parker	

Chapter 15.....	337
Immuno-Gene Therapy for Metastatic Prostate Cancer	
Takefumi Satoh, Terry L. Timme, Yehoshua Gdor, Brian J. Miles, Robert J. Amato, Dov Kadmon, and Timothy C. Thompson	
Chapter 16.....	355
Distilling the Past – Envisioning the Future	
Richard J. Ablin and Malcolm D. Mason	
Index	399

Chapter 8

ORTHOTOPIC METASTATIC MOUSE MODELS OF PROSTATE CANCER

Robert M. Hoffman

Department of Surgery, UCSD Medical Center, San Diego, CA, USA and AntiCancer, Inc., San Diego, CA, USA

Abstract: Orthotopic metastatic models of prostate cancer are reviewed here. Emphasis is placed on surgical orthotopic implantation models in nude mice. The advantages of surgical orthotopic implantation of tissue fragments are discussed with regard to resulting metastasis which reflect the clinical pattern of prostate cancer. The use of green fluorescent protein and red fluorescent protein to image primary tumor growth and metastasis, including whole-body imaging of prostate cancer, is discussed. The application of the models for gene expression studies, drug discovery, and gene therapy is also reviewed.

Key words: prostate cancer cell lines, surgical orthotopic implantation, green fluorescent protein, red fluorescent protein, whole-body imaging, metastasis, drug discovery

1. BACKGROUND OF METASTATIC ANIMAL MODELS OF PROSTATE CANCER

Prostate cancer is the most frequently occurring tumor in men and is the second leading cause of male death in the United States, accounting for about 30,000 deaths per year in the U.S. (1). Huggins and Hodges (2) observed the androgen dependence of prostatic carcinoma growth, and since that time androgen ablation has been an important feature of therapy for prostate carcinoma. However, for prostate carcinomas that have become hormone-independent, there is no effective systemic treatment (3).

A clinical report of over 600 patients suffering from stage D2 prostate cancer indicated an overall mean survival of 36 months in patients treated with combined androgen blockade (4). At the time of initial presentation, approximately 30–50% of prostate cancer patients have evidence of metastatic disease (5). The mechanism controlling prostate cancer

progression and effective therapeutic strategies for metastatic prostate cancer are poorly understood. This is in part due to the lack of a suitable animal model that can mimic the clinical patterns of human prostate cancer growth and metastasis (6).

Prostate cancer occurs in a high percentage of men over 50 but is aggressive in only a small percentage of patients. It is, therefore, also necessary to develop models and markers to distinguish aggressive from non-aggressive tumors, and responsive from non-responsive ones, in order to make proper treatment decisions (7) and to develop new treatment strategies (3).

Nonhuman mammals have very rare incidence of prostate cancer (8), which limit the possibilities of using nonhuman mammal models to study human prostate cancer. With the first introduction of immunodeficient rodents in cancer research in the late 1960s (9, 10), xenografted human cancer models are now widely used. The inability to reject many of the xenografts implanted in these animals due to defect(s) in their immune system make them the only known tool for studying *in vivo* human cancer growth and metastasis outside the human body (6, 9, 10).

A number of cell lines from human prostatic carcinoma that grow in athymic nude mice (SCID), including LNCaP which is androgen-dependent (11), and the androgen-independent cell lines DU-145 (12) and PC-3 (13, 14) have been isolated (3). The Dunning R-3327 hormone-dependent rat prostatic adenocarcinoma has also been developed (15).

Experimental *in vivo* growth of human prostate carcinoma lines has usually followed subcutaneous (s.c.) transplantation, with occasional metastatic activity, as first observed by Ware et al. (16). Ware et al. (17) were the first to demonstrate that differential injection sites affected the behavior of PC-3. Intrasplenic injection (18) resulted in metastatic activity. The PC-3 line originated from a bone metastasis (4). When PC-3 was injected into the tail vein of the nude mice while the inferior cava was occluded, tumor growth in the lumbar vertebrae, pelvis, and femurs occurred (19). When PC-3 cells were injected into the peritoneal cavity, intra-abdominal growth resulted; when injected into the spleen, liver metastases resulted and when injected into the seminal vesicles, large tumors developed from there (20), when injected intracardially, bone metastasis could also result (19, 20, 21).

LNCaP is a cell line derived from a supraclavicular lymph node metastasis of human prostate carcinoma. LNCaP exhibits increased proliferation in response to androgens. When LNCaP cells were mixed with the reconstituted basement membrane matrigel and injected S.C. in nude mice, tumors grew in the mice by 12 weeks without observed metastases (22).

More realistic models of human cancer can be constructed through orthotopic transplantation of the human tumor to the animal host (23). Subsequent studies in a number of laboratories have shown that orthotopic injection of human tumor cells in immunodeficient mice can produce relevant metastatic patterns in comparison to ectopic transplantation (24–30).

The tumorigenicity and the incidence of metastasis of LNCaP after orthotopic (intraprostate) or S.C. injection in male nude mice were compared by Stephenson et al. (31). LNCaP cells produced tumors only when orthotopically implanted in the prostate. Viewig et al. (32) showed that orthotopic implantation of the rat R3327-MatLyLu prostate adenocarcinoma in Copenhagen rats resulted in tumor growth in the prostate and metastasis to pelvic and retroperitoneal lymph nodes and lung.

In a subsequent study by Pettaway et al. (33), 56% of nude mice injected orthotopically with a suspension of LNCaP cells formed prostate tumors. Twelve of 43 mice had microscopic metastases in the regional lymph nodes.

In another study, orthotopic injection of LNCaP in nude mice resulted in local growth in 7 of 10, and lymph node metastasis in 4 of 10 nude mice (34).

Hormone-independent cell lines (PC-3, PC-3-125-IL, and TSU-Pr1) were highly tumorigenic and had a higher rate of lymph node metastasis after orthotopic injection than after S.C. implantation. PC-3 cell lines consistently metastasized to the lungs (34).

Nude and SCID mice were injected either S.C. or orthotopically with LNCaP cell suspensions in a comparative study by Sato et al. (35). LNCaP tumor incidence after S.C. injection was 100% in SCID mice and 80% in nude mice. No lymph node or distant metastases were observed with S.C. tumors. After orthotopic injection in SCID and nude mice retroperitoneal or mediastinal lymph node metastases were found in 100% of SCID mice, and microscopic pulmonary metastases were identified in 40%. The nude mice had retroperitoneal lymph node metastasis in 25% of the animals but no other metastasis was found.

Thalmann et al. (36) reported a spontaneous bone metastasis model of androgen-independent human prostate cancer LNCaP derived sublines. The animals developed bone metastasis in 10% and 21.5% of intact and castrated hosts, respectively, after orthotopic injection of cell suspensions. These results provided some useful information to recognize the biological behavior of prostate cancer.

Transrectal ultrasonography (TRUS) was used to monitor mouse orthotopic prostate tumors. Orthotopic tumors were initiated by inoculation of RM-9 murine prostate cancer cells into the dorsal prostate of C57BL/6 male mice. By ultrasound, tumors became detectable 7 days after tumor

cell inoculation. The tumor volume calculated by TRUS correlated significantly with the actual tumor weight measured at autopsy. Similarly, tumor growth suppression induced by cis-diamminedichloroplatinum (CDDP) was detected by TRUS with reasonable accuracy (37).

Injection of tumor cells into the prostate gland of nude mice, however, requires delicate, hard-to-control technical conditions, and spillage outside the prostate may generate rather variable results. Furthermore, some studies showed that artificial dissemination rather than spontaneous metastasis might occur following tumor cell injection, even when cells were not directly injected into the vasculature (38–40). It has been shown that tumor cells can enter the draining lymph or blood circulation within 10 minutes to 3 hours of injection, which will eventually form distant artificial metastases (41, 42). Most importantly, a cell suspension lacks tissue architecture, which seems critical for the full expression of the spontaneous metastatic potential of the transplanted human tumors.

Previous studies showed that the proliferation of tumor cells implanted in nude mice was preceded by the penetration of host stromal cells into the tumor (43, 44). Based on this important role of stroma in tumor growth, some investigators coinjected cultured fibroblasts with tumor cells and observed significant, growth-stimulating effects (45–47). Also, many studies demonstrated enhanced growth of tumor cells following co-injection of Matrigel (48–51), an extract of basement membrane components, which primarily consists of laminin, collagen IV and heparan sulfate proteoglycan (52). Current concepts suggest that Matrigel serves as a supportive matrix for the tumor cells. It collects tumor cells, allows paracrine factors to take effect, activates the release of angiogenic factors and stimulates the production of proteases and motility of tumor cells, thus facilitating growth and progression (53, 54).

We have developed surgical orthotopic-implantation (SOI) techniques utilizing histologically intact tissue, including surgical specimens, to develop metastatic models in immunodeficient mice for most types of human cancer including colon cancer (55, 56), human bladder cancer (57, 58), human lung cancer (59–62), and human pancreatic cancer (63). Surgical orthotopic implantation of histologically intact tumor tissue maintains the overall tissue architecture during implantation.

The histologically intact tumor tissue used in SOI possesses a large amount of supportive stromal cells, which are essential for maintaining the three-dimensional tumor architecture. The tissue architecture is believed to contribute to the difference in metastatic expression resulting from SOI and orthotopic injection of tumor cell suspensions, which have no three-dimensional architecture.

For all cancer types tested, intact-tissue orthotopic transplantation resulted in greater metastatic expression than orthotopic transplantation of cell suspensions (3, 55, 57, 58, 63–67).

We demonstrated orthotopic growth of prostate cancer line PC-3 with subsequent lymph node metastases by using the SOI technique (3). In a subsequent study, a large series of animals was implanted with PC-3 by improved SOI techniques (6). The patterns of growth and metastasis represented clinical prostate cancer. The advantages of this model for the study of prostate cancer and the possible mechanisms that underlie them are discussed below.

The early stages of tumor progression and micrometastasis formation have been difficult to visualize in current models due to the inability to identify small number of tumor cells against a background of many host tissues. We have developed new models of human and animal cancer by transfer of the *Aequorea victoria* jellyfish green fluorescent protein (GFP) gene to tumor cells that enabled visualization of fluorescent tumors and metastases at the microscopic level in fresh viable tissue and *in vivo* after transplantation (68–73), including prostate cancer (74). These models are discussed below.

2. DESCRIPTION OF METASTATIC PROSTATE CANCER MODELS

2.1 Orthotopic Models Implanted with Tumor-Cell Suspensions

Stephenson et al. (31), as mentioned above, reported lymph node metastasis but no lung metastasis of PC-3 after orthotopic injection of cell suspension in nude mice.

The tumorigenicity of and the incidence of metastasis of human prostate cancer PC-3M and LNCaP-FGC (LNCaP) cell lines subsequent to prostatic (orthotopic) or S.C. (ectopic) implantations in male nude mice was also determined (31). LNCaP cells produced tumors only in the prostate. Enhanced tumorigenicity at the orthotopic site was found for PC-3M cells, but not parental PC-3. Lymph node metastases were observed in practically all mice given an injection of PC-3M cells in the prostate, but they were uncommon with S.C. injection of these cells. LNCaP tumors in the mouse prostate (but not PC-3M tumors) produced detectable levels of human prostate-specific antigen (PSA) in the serum, even when tumors were

small (1.5 mm in diameter). Immunohistochemistry analysis demonstrated the presence of the PSA marker in tissue sections of LNCaP but not of PC-3M tumors (31).

Previous studies have shown, as mentioned above, that the injected tumor cells may enter the lymphatic stream very shortly after injection (38–42). Therefore, the metastasis observed may be due to artificial dissemination.

Shevrin et al. (20) demonstrated lung metastasis of PC-3 cells, but this was achieved by injecting tumor cells directly into the tail vein of the nude mice, in which several steps of the metastatic process that naturally occur in patients were bypassed (75–77). Waters et al. (78) reported rather high lung metastasis of PC-3 cells after urinary bladder wall injection of cell suspensions. However, they concluded, on the other hand, that lung metastasis of PC-3 from orthotopic tumor cell injection was infrequent (1 of 10 mice).

Pettaway et al. (33) demonstrated that cells derived from the metastatic lesions of the orthotopically injected parental line of LNCaP, became increasingly metastatic after multiple selection cycles of orthotopic injection, subsequent isolation of metastatic cells and orthotopic reinjection. Even so, after a number of cycles of selection LNCaP still did not metastasize to the lung from the orthotopic site. Lung metastasis was only achieved by iv injection of the selected metastatic cells. Variants with increasing metastatic potential of PC-3M and LNCaP cells were selected by injection into the prostates of athymic mice. Tumors from the prostate or lymph nodes were harvested, and cells were reinjected into the prostate. This cycle was repeated three to five times to yield cell lines PC-3M-Pro4, PC-3M-LN4, LNCaP-Pro3-5, and LNCaP-LN3-4. Parental and variant cells were injected into the prostates of nude mice. PC-3M-LN4 cells produced enhanced regional lymph node and distant organ metastasis as compared to PC-3M-Pro4 or PC-3M cells. Orthotopically implanted LNCaP-LN3 cells produced a higher incidence of regional lymph node metastases than LNCaP-Pro5 or LNCaP cells. The metastatic LNCaP-LN3 cells exhibited clonal karyotypic abnormalities, were less sensitive to androgen (*in vitro* and *in vivo*), and produced high levels of PSA (33).

Histopathologic evidence from a murine prostate gland into which SP 3031 human prostate cancer cells had been injected indicated dysplastic glandular epithelium and carcinomatous areas. The human prostate tumors transformed host organ cells, with specific chromosomal alterations that may be associated with transformation (79).

Murine prostate cell lines were evaluated for growth and metastasis in orthotopic (dorso-lateral prostate) locations. Orthotopic tumors produced by cell lines derived from metastatic lesions tended to grow less rapidly but

demonstrated greater spontaneous metastatic potential than the cell lines derived from primary tumors (80).

2.2 Surgical Orthotopic Implantation (SOI) of PC-3 in the Nude Mouse Prostate

The hormone-independent human prostate cancer line PC-3 was SOI as intact tissue which was harvested from nude-mouse S.C.-growing tissue (3). The orthotopic transplantation resulted in local growth and metastasis to the bladder and kidney, as well as distant metastasis to the inguinal, iliac, and mediastinal lymph nodes. Hydronephrosis was observed due to urinary blockage by the locally-growing tumor. The human genomic probe demonstrated by in situ hybridization that the tumors were of human origin showing a positive hybridization stain for the tumor cells but not for the stroma or lymphocytes, in the nude mouse lymph-node metastasis of PC-3. The histology of DU-145 and PC-3 growing and metastasizing in the nude mice matched published histologies of these tumors (12, 19). This orthotopic transplant model of prostate carcinoma resembled the clinical picture of growth within the prostate capsule, showing urinary obstruction, hydronephrosis, local invasion, and distant metastasis (3).

Using improved SOI of PC-3 in the ventral portion of the prostate (6), the take rate was 95% with only 1 of 20 mice having no orthotopic growth upon autopsy. Within the 3-month period following implantation, all tumors in the prostate reached more than 2 cm in diameter and usually disfigured the shape of the lower abdomen. The survival time of the animals ranged from 9 to 12 weeks. At time of euthanization, severe signs of cachexia could be observed in all the mice. Autopsy demonstrated that the orthotopically growing tumor usually protruded into the abdominal cavity and very frequently invaded the lower abdominal wall. Distended urinary bladder and hydronephrosis due to blocked urethras were also frequently seen. The seminal vesicles, the bladder, and the lower abdominal wall were often invaded by the orthotopic primary tumors. Microscopic examination of the tissue sections demonstrated that 5 of 19 animals had lung metastases and 13 of 19 had periaortic lymph node metastases (6). Histopathology of the primary tumor showed sheets of densely packed, anaplastic epithelial cells with abundant, foamy, eosinophilic cytoplasm. The nuclei were pleomorphic and had varying amounts of unevenly dispersed chromatin. Many abnormal mitoses could be seen. The prostate gland was almost replaced by tumor cells and very few glandular structures could be seen (6). Microscopically, lymph node metastases were characterized by widespread infiltration of tumor cells in the subcapsular, the cortical and medullary area. In many

of the lymph nodes analyzed, tumor cells occupied the whole node and lymphatic cells could barely be seen.

Microscopic examination of lung specimens showed that the metastases were disseminated. Small nests of tumor cells were observed in almost every high power field. When large tumor nests were seen, they often resided around the airway structures (6).

Intact tissue of the human prostate carcinoma cell line PC-3M was prepared by growth of this cell line subcutaneously in a nude mouse. One piece of 1.5 mm³ intact tumor tissue was implanted by SOI in the ventral lateral lobes of the prostate gland of 10 nude mice. All 10 mice had tumors in the prostate gland and metastasis to periaortic lymph nodes. The time when mice with implanted PC-3M become moribund was 28–32 days after SOI (81).

2.3 Surgical Orthotopic Implantation of LNCaP in the Nude Mouse Prostate

LNCaP grew extensively after SOI in the ventral portion of the prostate. Eighteen of 20 implanted mice had orthotopic growth. Autopsy demonstrated that the orthotopically-growing tumors usually protruded into the abdominal cavity and very frequently invaded the lower abdominal wall. Distended urinary bladder and hydronephrosis due to blocked urethra were also frequently seen. The seminal vesicles, the bladder, and the lower abdominal wall were often invaded by the orthotopic primary tumors. Microscopic examination of the tissue sections demonstrated that 8 of 18 animals had lung metastases and 11 of 18 had periaortic lymph node metastases. Histopathology of the primary tumor showed densely packed, poorly differentiated cells. The prostate gland was almost replaced by tumor cells and very few glandular structures could be seen. Microscopically, lymph node metastases involved almost the whole node. Microscopic examination of lung specimens showed that the metastases were disseminated in small nests of tumor cells. The mean survival time of the animals was 72 days (82).

SOI eliminated the need to select highly metastatic cells through complex procedures from a parental tumor for the purpose of establishing metastatic animal models of human cancer as was necessary for the orthotopic models using cell suspensions, described above. Moreover, the SOI metastatic models more closely mimic the clinical pattern, thus providing better tools to study the biology of cancer metastasis and for evaluating novel therapeutics for prostate cancer (6).

2.4 Bone Metastasis Models of Prostate Cancer

Thalman et al. (36) injected a mixture of human fibroblasts and LNCaP human prostate carcinoma cells into the dorsolateral lobe of the prostate gland of athymic mice. Metastases were selected that were apparently hybrids of the human fibroblasts and cancer cells. These variants developed bone metastasis in 10% and 21.3% of intact and castrated hosts, respectively.

A number of experimental bone metastasis models have also been developed in the last several years (19–21, 73). To establish these models, a high metastatic cell line was first selected and inoculated via the tail vein. In one study, in order to detect bone marrow metastases, isolation of total RNA from the bone marrow and subsequent RT-PCR was necessary (73). These types of models provide a useful tool for prostate cancer, but they do not mimic the natural history of this disease.

Using GFP-expressing PC-3 transplanted by SOI to the dorsolateral lobes of the nude mouse prostate, we established an imageable spontaneous bone metastasis mouse model of non-selected human prostate cancer. In this model, the GFP expression of the SOI-implanted PC-3 cell line enabled metastases to be visualized throughout the skeletal system and to other important organs as well. Extensive and widespread skeletal metastases, visualized by GFP expression, were found. The skeletal metastasis included the skull, rib, pelvis, femur, and tibia.

Metastases in the transplanted animals were also found in the lung, pleural membrane, liver, kidney, adrenal gland, brain and spinal cord. Thus, the metastatic pattern of human prostate cancer PC-3-GFP accurately reproduces the clinical course of advanced metastatic androgen-independent prostate cancer (74). These data demonstrate the far-reaching malignancy of this tumor (74).

Such a high incidence of skeletal and other metastases could not have been previously visualized before the development of the GFP-SOI model which provided the necessary tools. The bone microenvironment in the mouse provides a highly fertile soil for human prostate cancer matching the clinical situation (83). The PC-3-GFP model also revealed for the first time the extensive spontaneous liver metastasis potential of this tumor. This new metastatic model will be useful for studying the mechanism and developing therapy of skeletal and other metastases in prostate cancer (74).

The green fluorescent protein (GFP) gene was introduced into LNCaP cells by lipofection (84). Biological characteristics of a subline (LNCaP-GFP) that expressed GFP at high level were compared to those of the parental cells. LNCaP-GFP cells were orthotopically inoculated to the SCID

mouse, and metastases to distant organs were chronologically examined under fluorescence microscopy. There was no difference in growth rates and androgen-responsiveness *in vitro* between LNCaP-GFP and LNCaP cells. LNCaP-GFP cells inoculated to SCID mice produced prostate specific antigen. Colonies consisting of a few LNCaP-GFP cells were detected in the lung under fluorescence microscopy as early as 4 weeks after orthotopic inoculation (84).

3. GENE EXPRESSION AND PROSTATE CANCER METASTASIS MODELS

A prostate cancer line (PC-3M) was engineered to overexpress hyaluronidases (hyal-1). Although the *in vitro* properties of the hyal-1 overexpressing cell line was indistinguishable from the parental cells, the orthotopic growth of hyal-1 expressing PC-3M cells in *nu/nu* mice resulted in significantly increased numbers of metastases, suggesting a role for hyal-1 in extravasation and metastasis (85).

The nuclear factor (NF)-kappaB/relA transcription factor is constitutively activated in human prostate cancer cells. It was determined that blocking NF-kappaB/relA activity in human prostate cancer cells affected their angiogenesis, growth, and metastasis in an orthotopic nude mouse model of PC-3M. Transfection with a mutated IkappaBalpha (IkappaBalphaM) blocks NF-kappaB activity. PC-3M control cells produced rapidly growing tumors and regional lymph node metastasis, whereas PC-3M-IkappaBalphaM cells produced slow-growing tumors with low metastatic potential. Inhibition of NF-kappaB inhibited expression of three major proangiogenic molecules, vascular endothelial growth factor (VEGF), interleukin (IL)-8, and matrix metalloproteinase (MMP)-9, and decreased tumore angiogenesis (86).

Subclones of the PC-3M and LNCaP cell lines were selected for increased metastatic potential after successive orthotopic implantation in the prostate of nude mice. Comparative genomic hybridization (CGH) was used to compare the chromosomal abnormalities between the parental cell lines and variants to determine whether specific chromosomal abnormalities can be associated with different growth properties. PC-3M-Pro4, a derivative line that produced significantly larger tumors in the prostate, had a unique gain of 3q13. PC-3M-LN4, a derivative line that produced significantly larger metastatic tumors in the lymph nodes and had higher incidences of distant metastases, had a specific gain of 1q21-q22 and losses of 10q23-pter and 18q12-q21. A derivative line of LNCaP that produced significantly larger tumors in the prostate, LNCaP-Pro5, had a unique gain on 13q12-q13. In comparison, LNCaP-LN3, a derivative line that had a significantly

higher incidence of lymph node metastases and produced significantly larger metastatic tumors in the lymph nodes, had specific losses of 16q23–qter and 21q (87).

To investigate the potential genetic changes underlying the progression of human hormone-resistant prostate cancer, chromosomal alterations of the DU-145 cell line and a subline isolated from a metastasis in an orthotopic model were analyzed. DU-145 cells were injected into the dorsal prostate. From a resulting paraaortic lymph node metastasis, a subline (DU-145 MN1), was isolated. After orthotopic implantation of DU-145 cells tumorigenicity was 100% but only 2 mice had lymphnode metastases. In contrast, the take rate after implantation of DU-145 MN1 was 100%, with frequent lymphnode metastases. There was gain of a chromosome 8 and only two copies of chromosome 17 in the DU-145 MN1 cells as compared to the parental cell line. The emergence of an i(9)(q10) in addition to two normal chromosome 9 homologues in the DU-145 MN1 cell line was confirmed by fluorescent *in situ* hybridization (FISH) using a chromosome 9-specific painting probe. Chromosomal changes, following repeated orthotopic implantation, may enable location of the genes involved in the progression and chemoresistance of human hormone-resistant prostate cancer (88).

After orthotopic intraprostatic injection of tumor cells into SCID mice, the metastatic DU-145 prostate carcinoma cells expressed 12-lipoxygenase (12-LOX) at a significantly higher level compared with the non-metastatic counterparts. The functional involvement of 12-LOX in the metastatic process was demonstrated when DU-145 cells were pretreated *in vitro* with the 12-LOX inhibitors N-benzyl-N-hydroxy-5-phenylpentamide (BHPP) or baicalein with subsequent inhibition of lung colonization in the orthotopic model (89).

IL-8 expression by human prostate cancer growing within the prostate of athymic nude mice regulates tumor angiogenesis, growth, and metastasis. Poorly metastatic PC-3P cells were transfected with the full-length sense IL-8 cDNA, whereas highly metastatic PC-3M-LN4 cells were transfected with the full-sequence antisense IL-8 cDNA. After orthotopic implantation, the sense-transfected PC-3P cells were highly tumorigenic and metastatic, with significantly increased neovascularity and IL-8 expression compared with either PC-3P cells or controls. Antisense transfection significantly reduced the expression of IL-8 and MMP-9 and tumor-induced neovascularity, resulting in inhibition of tumorigenicity and metastasis. These results demonstrate that IL-8 expression regulates angiogenesis and metastasis in prostate cancer, in part by induction of MMP-9 expression (90).

Human prostate PC-3 ML tumor cells transfected with IL-10 were examined for tumor growth and metastasis following orthotopic implantation

in the prostate gland of SCID mice. Volume and extent of metastasis were negatively correlated with the amount of IL-10 production. Controls showed that parental PC-3 ML grew rapidly and metastasized when implanted orthotopically and died by 14–16 weeks. In contrast, the PC-3 ML-IL10a or PC-3 ML-IL10b clones induced only 10–20% death after 23–24 weeks (91).

Transfection of primary human prostate tumor cell lines (HPCA-10a, 10b, 10c, and 10d) with the transforming growth factor (TGF)-beta-1 gene promoted tumor growth, angiogenesis, and metastasis after orthotopic implantation in SCID mice. In contrast, IL-10 transfected cells or cells co-transfected with these two genes exhibited reduced growth rates and significantly reduced angiogenesis and metastasis. TGF-beta1 expression induced MMP-2 expression, whereas IL-10 down-regulated MMP-2 expression while up regulating tissue inhibitor of matrix metalloproteinase (TIMP)-1 in the transfected cells. Mouse survival was zero after 4–6 months in mice bearing transforming growth factor-beta1 (TGF- β 1) and MMP-2-expressing tumors. Survival increased significantly in mice implanted with IL-10- and TIMP-1-expressing tumors (92).

Prostate adenocarcinoma PC-3 and DU-145 cell lines express alphaII(b)beta3 integrin markers. Implantation in SCID mice determined that alphaII(b)beta3 mediates metastasis. In DU-145 cells the integrin localizes to focal contact sites, whereas it is predominantly intracellular in PC-3 cells. Both tumor cell lines were tumorigenic when implanted subcutaneously or intraprostatically in SCID mice, but only DU-145 cells injected intraprostatically metastasized. There was higher expression of alphaII(b)beta3 in DU-145 tumor cell suspensions isolated from the prostate when compared to DU-145 tumor cells from the subcutis (93).

A nontumorigenic cell line isolated from the rat prostatic epithelium (NbE) transfected with the activated oncogene p185neu-T was used to investigate the role of this oncogene in tumor progression. When clones overexpressing p185neu-T were injected orthotopically into the dorsal-lateral prostates of nude mice, prostatic tumors were detected in all mice injected and metastasis was detected to the skeletal muscle in the rib area in 60–80% of the mice injected. Control cell lines produced no prostatic tumors or metastases. Clones overexpressing p185neu-T demonstrated an increased expression of epidermal growth factor receptor and p180erbB4 (94).

The expression level of several metastasis-regulating genes correlated with the metastatic potential of human prostate cancer cells implanted into the prostate of nude mice. Human PC-3M cells and selected cell variants with different metastatic potentials were evaluated. Human prostate cancer cells implanted in nude mice at an ectopic site (S.C.) expressed lower levels

of epidermal growth factor receptor (EGFR), multidrug resistance (mdr)-1, basic fibroblast growth factor (bFGF), IL-8, and collagenase type IV than those implanted in an orthotopic site, indicating that the expression of these genes was dependent on the organ environment. Highly metastatic cells growing in the prostate expressed higher levels of EGFR, bFGF, type IV collagenase, and mdr-1 mRNA than low metastatic parental cells in the same site (95).

4. GENE THERAPY AND PROSTATE CANCER METASTASIS MODELS

Angiogenin, a mediator of neovascularization was targeted by an antisense oligodeoxynucleotide, designated JF2S, in human prostate tumors in nude mice in an orthotopic model. Systemic prophylactic administration of JF2S prevented, in 47% of mice, formation of regional iliac lymph node micrometastases arising from primary PC-3 tumors growing orthotopically in the prostate. Total protection from regional metastasis occurred in those mice in which JF2S diminished human angiogenin expression. Tumor angiogenesis was also impaired by JF2S treatment. These findings demonstrate that human prostate cancer metastasis in athymic mice is susceptible to disruption of human angiogenin gene expression (96).

The effects of interferon-beta (IFN-beta) gene transfer on the growth of PC-3MM2 human prostate cancer in nude mice were investigated. Intratumoral delivery of an adenoviral vector encoding murine IFN-beta (AdIFN-beta) suppressed orthotopic PC-3MM2 tumors and development of metastasis by 80%, and eradicated the tumors in 20% of mice. Immunohistochemical staining showed that AdIFN-beta-treated tumors contained fewer microvessels, fewer proliferating cells, and more apoptotic cells than did the control tumors. Compared with controls, tumors injected with AdIFN-beta expressed higher levels of IFN-beta and inducible nitric oxide synthase (iNOS) and lower levels of basic bFGF and TGF- β 1 (86).

Highly metastatic PC-3M human prostate cancer cells were engineered to constitutively produce murine IFN-beta with a retroviral vector containing murine IFN-beta cDNA. Parental (PC-3M-P), control vector-transduced (PC-3M-Neo), and IFN-beta-transduced (PC-3M-IFN-beta) cells were injected into the prostate or subcutis of nude mice. PC-3M-P and PC-3M-Neo cells produced rapidly growing tumors and regional lymph node metastases, whereas PC-3M-IFN-beta cells did not. PC-3M-IFN-beta cells

also suppressed the tumorigenicity of bystander non-transduced prostate cancer cells. PC-3M-IFN-beta tumors were homogeneously infiltrated by macrophages, whereas control tumors contained fewer macrophages at their periphery. PC-3M-IFN-beta tumors contained fewer proliferative cells and more apoptotic cells than controls. Staining with antibody against CD31 showed that control tumors contained more blood vessels than PC-3M-IFN-beta tumors. The data suggested that the suppression of tumorigenicity and metastasis of PC-3M-IFN-beta cells was due to inhibition of angiogenesis and activation of host effector cells (97).

The efficacy of a single injection of a recombinant adenovirus expressing murine IL-12 (AdmIL-12) was determined by direct injection into orthotopic mouse prostate carcinomas generated from a poorly immunogenic cell line (RM-9) derived from the mouse prostate reconstitution system. Significant growth suppression and increased mean survival time were observed compared with controls. Suppression of pre-established lung metastases was also observed. Cytolytic natural killer cell activity was markedly enhanced 1–2 days after virus injection. Immunohistochemical analysis showed significantly elevated intratumoral infiltration of CD4+ and CD8+ T-cells. Splenocyte-derived cytotoxic T-lymphocytes were also detected. Increased numbers of nitric oxide synthase-positive macrophages were also seen in the AdmIL-12 treated group. The antitumor efficacy of adenovirus-mediated IL-12 depends on the activation of nitric oxide synthase in macrophages and T-cell activation (98).

The effectiveness of an adenovirus that expresses both IL-12 and the costimulatory molecule B7-1 (AdmIL12/B7) or one that expresses IL-12 alone (AdmIL-12) were compared using the poorly immunogenic RM-9 orthotopic murine model of prostate cancer. A significant reduction in orthotopic tumor size and increased survival was demonstrated in mice treated with a single orthotopic injection of AdmIL-12/B7 compared with AdmIL-12 or controls. Orthotopic treatment of tumors with both vectors led to an infiltration of both CD4+ and CD8+ immunoreactive cells, with AdmIL-12/B7 treatment having a more prolonged infiltration of CD8+ cells. AdmIL-12/B7 was also more effective than AdmIL-12 or controls at suppression of pre-established metastases. A vaccine model based on s.c. injection of infected, irradiated RM-9 cells demonstrated that both AdmIL-12 and AdmIL-12/B7 were effective at suppressing the development and growth of challenge orthotopic tumors (99).

Mutation of the p53 tumor suppressor gene has been associated with the progression of prostate cancer. An orthotopic metastatic model for human prostate cancer was used to determine efficacy of the wild-type p53 gene using an adenoviral vector (rAd-p53). The human prostate cancer cell line

PC-3 has a homozygous loss of p53 expression in nude mice following orthotopic injection. A single injection of rAd-p53 into an established orthotopic prostate tumor resulted in primary tumor growth suppression and reduced the frequency of metastasis (100).

An orthotopic mouse model of metastatic prostate cancer using a cell line (RM-1) derived from the mouse prostate was developed. Adenovirus (ADV)-mediated transduction of the herpes simplex virus thymidine kinase (HSV-tk) gene in conjunction with ganciclovir (GCV) in this model led to significant suppression of growth and of spontaneous metastasis with a significant survival advantage and a continued suppression of metastatic activity for treated animals despite regrowth of the primary tumor (101).

Induction of potent antitumor natural killer (NK) cell activity by herpes simplex virus-thymidine kinase and ganciclovir therapy was observed in the orthotopic RM-1 mouse model of prostate cancer. *In vivo* depletion of NK cells resulted in a 20% reduction in growth suppression within the primary tumor and complete abrogation of the inhibition of preestablished lung metastases. Depletion of T-cells had no effect on either response. NK cells within adenovirus/HSV-tk- and ganciclovir-treated tumors, thus mediated both local and systemic antitumor activities in this model (102).

5. OTHER TREATMENT OF PROSTATE CANCER METASTASIS

Arsenic trioxide (As₂O₃) was administered to SCID mice inoculated orthotopically with PC-3 cells. The orthotopic metastasis model showed tumor growth inhibition in the primary and metastatic lesions with no signs of toxicity (103).

Caveolin-1 plays important roles in signal transduction and lipid transport. Injections of caveolin-1 antibody suppressed the orthotopic growth and spontaneous metastasis of a highly metastatic, androgen-insensitive caveolin-1-secreting mouse prostate cancer (104).

Prostate stem-cell antigen (PSCA) is a cell-surface antigen expressed in normal prostate and overexpressed in prostate cancer tissues. Anti-PSCA mAbs efficacy was evaluated on the androgen-dependent LAPC-9 and the androgen-independent recombinant cell line PC-3-PSCA. Orthotopic tumors were inhibited in a dose-dependent manner. Inhibition of metastasis to distant sites also occurred resulting in a significant prolongation in the survival of tumor-bearing mice (105).

6. ORTHOTOPIC DOG MODEL

A new canine prostate cancer epithelial cell line designated DPC-1 has been isolated from a poorly differentiated canine prostatic adenocarcinoma (106). Tumorigenicity was assessed in nude mice and in one adult immunodeficient dog. DPC-1 displays immunoreactivity to human PSA and prostate-specific membrane antigen (PSMA). DPC-1 was found to be highly tumorigenic not only in nude mice but also for the first time after orthotopic seeding in an immunodeficient dog.

7. MATERIALS AND METHODS IN THE AUTHOR'S LABORATORY

7.1 Animals

Outbred nu/nu mice, 4-6 weeks old, were used for s.c. and orthotopic transplantation of DU-145, PC-3, and LNCaP. All the mice were maintained in a pathogen-free environment. Cages, bedding, food, and water were autoclaved and changed regularly. All the mice were maintained in a daily cycle of 12 hr light and 12 hr darkness (3). They were maintained in a specific pathogen-free environment in compliance with USPHS guidelines governing the care and maintenance of experimental animals under Assurance Number A3873-01. Mice were fed with autoclaved laboratory rodent diet (Teklad LM-485, Western Research Products, Orange, CA) (6).

7.2 Surgical Orthotopic Implantation

PC-3 DU-145 and LNCaP cells were obtained initially from the American Tissue Type Culture Collection (Rockville, MD). Tumor tissue used for surgical orthotopic implantation was derived from a tumor growing subcutaneously after injection of prostate cancer cells in a nude mouse. Tissue from the periphery of the tumor was harvested in log phase and necrotic tissue was carefully removed under a dissecting microscope to minimize the amount of viable tissue for implantation. The viable tissue was then cut into small cubes of 1 mm³ in standard tissue culture medium under sterile conditions. To minimize variation in subsequent tumor growth and metastasis, these tumor pieces were randomly mixed and an equal amount of pieces was implanted in each mouse as described below.

7.2.1 SOI to Ventral Lateral Lobes of Prostate

Mice were anesthetized by isoflurane (Ohmeda Caribe Inc., Guayama, PR) and positioned supinely. An opening was made right above the pubis symphysis to expose the prostate gland. The fascia surrounding the ventral portion of the prostate was carefully isolated and the two ventral lateral lobes of the gland were separated by a small incision using a pair of fine surgical scissors. Five of the above tissue pieces were sutured into the incision using an 8-0 nylon suture. The two parts of the separated lobes were then sutured together with the tumor pieces wrapped within. The surrounding fascia was then used to wrap this portion of the gland to consolidate the incision. The abdomen was closed using a 6-0 suture (6).

7.2.2 SOI to Dorsal Lateral Lobe of Prostate

Two tumor fragments (1 mm^3) from a S.C. tumor from a single animal were implanted by SOI in the dorsolateral lobe of the prostate in nude mice. After proper exposure of the bladder and prostate following a lower midline abdominal incision, the capsule of the prostate was opened and the two tumor fragments were inserted into the capsule. The capsule was then closed with an 8-0 surgical suture. The incision in the abdominal wall was closed with a 6-0 surgical suture in one layer (7, 8). The animals were kept under isoflurane anesthesia during surgery. All procedures of the operation described above were performed with a $7 \times$ magnification microscope (Olympus) (74).

To confirm the human origin of the tumors growing in the nude mice, the Oncor total-human-genome probe (Oncor, Gaithersburg, MD) was used. Briefly, paraffin-embedded blocks of the nude-mouse tumor, both local and metastatic, were cut into $4\text{-}\mu\text{m}$ -thick sections and applied to silanized slides. After deparaffinization, protein digestion and dehydration, the Oncor biotinylated "Total-human DNA painting probe" was used for in situ hybridization. Avidin, anti-avidin antibody and horse-radish peroxidase-avidin complex with 3-3'-diaminobenzidine tetrahydrochloride (DAB) as the substrate was subsequently applied for the detection system according to the specifications supplied by Oncor. Hematoxylin was used in counterstaining. The nuclei of positive cells stained brown, indicating their human origin. Negative controls utilized the total procedure but without the human-genome-specific DNA probe. The human genomic probe was used to determine the human origin of the prostate tumors in the nude mice since neither DU-145 nor PC-3 produce PSA (3).

7.3 Histological and GFP Evaluation of Tumor Growth and Metastasis

Mice were euthanized if found moribund during the observation period. All mice were humanely sacrificed using CO₂ inhalation three months after tumor implantation and then immersed in 10% formalin for subsequent autopsy and microscopic examination. Regional and distant lymph nodes, the lung, the liver as well as other organs suspected of metastasis were routinely embedded, sectioned, and stained with hematoxylin and eosin using standard techniques for microscopic examination. The skeletal system was carefully examined grossly under a dissecting microscope (7×) with the removal of the soft tissue for possible bone metastasis (6).

7.3.1 GFP DNA Expression Vector

The RetroXpress vector pLEIN was purchased from Clontech Laboratories, Inc. (Palo Alto, CA). The pLEIN vector expresses enhanced green fluorescent protein (EGFP) and the neomycin resistance gene on the same bicistronic message which contains an IRES site (72).

7.3.2 Production of GFP Retrovirus

PT67, an NIH3T3-derived packaging cell line, expressing the 10 A1 viral envelope, was purchased from Clontech Laboratories, Inc. PT67 cells were cultured in DME medium (Irvine Scientific, Santa Ana, CA) supplemented with 10% heat-inactivated fetal bovine serum (FBS) (Gemini Bio-products, Calabasas, CA). For vector production, packaging cells (PT67), at 70% confluence, were incubated with a precipitated mixture of DOTAP™ reagent (Boehringer Mannheim), and saturating amounts of pLEIN plasmid for 18 hours. Fresh medium was replenished at this time. The cells were examined by fluorescence microscopy 48 hours post-transfection. For selection, the cells were cultured in the presence of 500 – 2000 μg/ml of G418 (Life Technologies, Grand Island, NY) for seven days (72).

7.3.3 GFP Gene Transfection of Prostate Carcinoma Cells

For GFP gene transfection, 20%-confluent PC-3 cells were incubated with a 1:1 precipitated mixture of retroviral supernatants of PT67 cells and Ham's F-12 K (GIBCO) containing 7% fetal bovine serum (FBS) (Gemini Bio-products, Calabasas, CA) for 72 hours. Fresh medium was replenished at this time. PC-3 cells were harvested by trypsin/EDTA 72 hours

post-transfection, and subcultured at a ratio of 1:15 into selective medium which contained 200 $\mu\text{g/ml}$ of G418. The level of G418 was increased to 1000 $\mu\text{g/ml}$ stepwise. PC-3 clones expressing GFP (PC-3-GFP) were isolated with cloning cylinders (Bel-Art Products, Pequannock, NJ) with trypsin/EDTA and were then amplified and transferred by conventional culture methods (74).

7.3.4 Doubling Time of Stable GFP Clones

PC-3-GFP or non-transfected cells were seeded at 1.5×10^4 in 35 mm culture dishes. The cells were harvested and counted every 24 hours using a hemocytometer (Reichert Scientific Instruments, Buffalo, NY). The doubling time was calculated from the cell-growth curve over a period of ten days (74).

7.4 Fluorescence Imaging

A Leica fluorescence stereo microscope model LZ12 equipped with a mercury 50W lamp power supply was used (107–109). To visualize both GFP and RFP fluorescence at the same time, excitation was produced through a D425/60 band pass filter and 470 DCXR dichroic mirror (110). Emitted fluorescence was collected through a long pass filter GG475 (Chroma Technology, Brattleboro, VT). Macroimaging was carried out in a light box (Lighttools Research, Encinitas, CA). Fluorescence excitation of both GFP and RFP tumors was produced through an interference filter 440+/-20 nm using slit fiber optics for animal illumination. Fluorescence was observed through a 520 nm long pass filter (110). Images from the microscope and light box were captured on a Hamamatsu C5810 3-chip cool color CCR camera (Hamamatsu Photonics Systems, Bridgewater, NJ).

Images were processed for contrast and brightness and analyzed with the use of Image Pro Plus 4.0 software (Media Cybernetics, Silver Springs, MD). High resolution images of 1024×724 pixels were captured directly on an IBM PC or continuously through video output on a high resolution Sony VCR model SLV-R1000 (Sony Corp., Tokyo Japan) (107–109).

8. CONCLUSIONS AND PERSPECTIVES

Intraprostatic implantation of PC-3 cell suspensions in nude mice resulted in paraaortic lymph node metastases in 10 of 10 mice with prostatic tumors, whereas metastases were present in only 2 of 9 mice after S.C. implantation. Tumorigenesis and metastasis were also 100% after subserosal implantation

of PC-3 cells within the wall of the urinary bladder. Subserosal implantation of PC-3 cells into the stomach wall also resulted in tumor formation and metastasis as well to regional lymph nodes in 100% of mice. In all experiments, regional lymph nodes were the most frequent site of metastasis, regardless of implantation site. The loss of organ specificity may have been due to use of cell suspensions instead of tumor fragments for orthotopic implantation (78, 111).

The invasive and metastatic behavior of metalloproteinase matrilysin transfected DU-145 cell lines injected into the dorsal lateral lobe of the prostate in SCID mice was compared to that observed when they are injected intraperitoneally. The results demonstrate that the level of mRNA expression of the matrilysin, stromelysin, TIMP-1, and TIMP-2 genes was similar at the two sites of injection. The invasive properties of DU-145 cells following orthotopic implantation were comparable to that observed on the diaphragm following intraperitoneal injection (112). Again this loss of host tissue specificity may have been due to use of cell suspensions instead of intact tissue fragments for orthotopic implantation. Further comparative experiments are necessary using the two techniques.

The use of GFP and now RFP allow unprecedented visualization of tumor growth *in vivo* including prostate cancer (74, 110). New techniques of *in vivo* imaging with these multicolor fluorescent reporters will enable important insight into the mechanisms of prostate cancer metastasis (110).

Recently transgenic models of prostate cancer have been developed, Gupta et al. (113) described the transgenic adenocarcinoma of the mouse prostate (TRAMP). In this model, expression of the SV40 early genes (T and t antigen, Tag) are driven by the prostate-specific promoter probasin which leads to cell transformation within the prostate. TRAMP mice develop prostate cancer without any chemical or hormonal treatment and metastasis to lymph nodes, lungs, liver, and bone occur over 12-28 weeks with median survival of 42 weeks. The potential question with these models is "what do they represent" since all cells express as an artificial transgene such as the SV40 T-antigens in the TRAMP model which is not the case in human prostate cancer.

REFERENCES

1. Jemal A, Thomas A, Murray T, Thun M. Cancer statistics, 2002. *CA Cancer J Clin* 2002, 52:23-47.
2. Huggins C, Hodges CV. Studies on prostatic cancer. I. The effects of castration, of estrogen and of androgen injections on serum phosphatases in metastatic carcinoma of the prostate. *Cancer Res* 1941, 1:293-7.

3. Fu X, Herrera H, Hoffman RM. Orthotopic growth and metastasis of human prostate carcinoma in nude mice after transplantation of histologically intact tissue. *Int J Cancer* 1992, 52:987-0.
4. Crawford ED, Eisenberger MA, McLeod DG, Spaulding JT, Benson R, Dorr FA. A controlled trial of leuprolide with and without flutamide in prostate carcinoma. *N Engl J Med* 1989, 321:419-24.
5. Stamey TA, McNeal JE. Adenocarcinoma of the prostate, In: *Campbell's Urology, 6th Ed.* Walsh PC, Retik AB, Stamey TA, Vaughn ED Jr., eds, Philadelphia: W.B. Saunders, 1992.
6. An Z, Wang X, Geller J, Moossa AR, Hoffman RM. Surgical orthotopic implantation allows high lung and lymph node metastatic expression of human prostate carcinoma cell line PC-3 in nude mice. *Prostate* 1998, 34:169-74.
7. Nakamoto T, Chang C, Li A, Chokak G. Basic fibroblast growth factor in human prostate cancer cells. *Cancer Res* 1992, 52:571-7.
8. Ware JL. Prostate tumor progression and metastasis. *Biochem Biophys Acta Rev Cancer* 1987, 907:279-98.
9. Arnold W, Kopf-Maier P, Micheel B, eds, *Immunodeficient Animals: Models for Cancer Research.* Basel: Karger, 1996.
10. Rygaard J, Povlsen CO. Heterotransplantation of a human malignant tumour to "nude" mice. *Acta Pathol Microbiol Scand* 1969, 77:758-60.
11. Horoszewicz J, Leong S, Kawinski E, Karr J, Rosenthal H, Chu T *et al.* Lncap model of human prostatic carcinoma. *Cancer Res* 1983, 43:1809-11.
12. Stone KR, Mickey D, Wunderli H, Mickey G, Paulson D. Isolation of a human prostate carcinoma cell line (DU-145). *Int J Cancer* 1978, 21:274-81.
13. Kaighn M, Narayan K, Ohnuki Y, Lechner J, Jones LW. Establishment and characterization of a human prostatic carcinoma cell line (PC-3). *Invest Urol* 1979, 17:1623.
14. Kozlowski J, McEwan L, Keer H, Sensibar J, Sherwood ER, Lee C *et al.* Prostate cancer, the invasive phenotype: Application of new in vivo, in vitro approaches, pp. 189-231. In: *Tumor Progression, Metastasis.* Fidler IJ, Nicholson G, eds, New York: Alan R. Liss, 1988.
15. Dunning WF. Prostate cancer in the rat. *Nat Cancer Inst Monogr* 1963, 12:351-69.
16. Ware JJ, Paulson DF, Mickey GH, Webb KS. Spontaneous metastasis of cells of the human prostate carcinoma cell line PC-3 in athymic nude mice. *J Urol* 1982, 128:1064-7.
17. Ware JL, Lieberman AP, Webb KS, Vollmer RT. Factors influencing phenotypic diversity of human prostate carcinoma cells metastasizing in athymic nude mice. *Exp Cell Biol* 1985, 53:163-9.
18. Sherwood E, Ford J, Lee C, Kozlowski J. Therapeutic efficacy of recombinant tumor necrosis factor alpha in an experimental model of human prostatic carcinoma. *J Biol Resp Mod* 1990, 9:44-52.
19. Shevrin Kukreja D, Ghosh S, Lad LT. Development of skeletal metastasis by human prostate cancer in athymic nude mice. *Clin Exp Metastasis* 1988, 6:401-9.
20. Shevrin D, Gorny K, Kukreja S. Patterns of metastasis by the human prostate cancer cell line PC-3 in athymic nude mice. *Prostate* 1989, 15:187-94.
21. Wu TT, Sike RA, Cui Q, Thalmann GN, Kao C, Murphy CF *et al.* Establishing human prostate cancer cell xenografts in bone: Induction of osteoblastic reaction by prostate-specific antigen-producing tumors in athymic and SCID/bg mice using Incap and lineage-derived metastatic sublines. *Int J Cancer* 1998, 77:887-94.

22. Lim DJ, Liu X, Sutkowski DM, Braun EJ, Lee C, Kozlowski JM. Growth of an androgen-sensitive human prostate cancer cell line, Incap, in nude mice. *Prostate* 1993, 22:109-1.
23. Wang WR, Sordat B, Piguet D, Sordat M. Human colon tumors in nude mice: Implantation site, expression of the invasive phenotype, pp. 239-45. In: *Immune-Deficient Animals. 4th Int. Workshop on Immune-Deficient Animals in Experimental Research*. Sordat B, ed., Basel: Karger, 1984.
24. Naito S, von Eschenbach AC, Glavazzi R, Fidler IJ. Growth and metastasis of tumor cells isolated from a human renal cell carcinoma implanted into different organs of nude mice. *Cancer Res* 1986, 46:4109-15.
25. Naito S, von Eschenbach AC, Fidler IJ. Different growth pattern and biologic behavior of human renal cell carcinoma implanted into different organs of nude mice. *J Natl Cancer Inst* 1987, 78:377-85.
26. Morikawa K, Walker SM, Jessup JM, Fidler IJ. *In vivo* selection of highly metastatic cells from surgical specimens of different primary human colon carcinoma implanted into nude mice. *Cancer Res* 1988, 48:1943-8.
27. Ahlering TE, Dubeau L, Jones PA. A new *in vivo* model to study invasion and metastasis of human bladder carcinoma. *Cancer Res* 1987, 47:6660-5.
28. Nakajima M, Morkawa K, Fabra A, Bucana CD, Fidler IJ. Influence of organ microenvironment on extracellular matrix degradative activity and metastasis of human colon carcinoma cells. *J Natl Cancer Inst* 1990, 82:1890-8.
29. Price JE, Polyzos A, Zhang RD, Daniels LM. Tumorigenicity and metastasis of human breast carcinoma cell line in nude mice. *Cancer Res* 1990, 50:717-21.
30. Giavazzi R, Campbell DE, Jessup JM, Cleary K, Fidler IJ. Metastatic behavior of tumor cells isolated from primary and metastatic human colorectal carcinomas implanted into different sites in nude mice. *Cancer Res* 1986, 46:1928-33.
31. Stephenson RA, Dinney CPN, Gohji K, Ordonez NG, Killion JJ, Fidler IJ. Metastatic model for human prostate cancer using orthotopic implantation in nude mice. *J Natl Cancer Inst* 1992, 84:951-7.
32. Vieweg J, Heston WDW, Gilboa E, Fair WR. An experimental model simulating local recurrence and pelvic lymph node metastasis following orthotopic induction of prostate cancer. *Prostate* 1994, 24:291-8.
33. Pettaway CA, Pathak S, Greene G, Ramirez E, Wilson MR, Killion JJ, Fidler IJ. Selection of highly metastatic variants of different human prostatic carcinomas using orthotopic implantation in nude mice. *Clin Cancer Res* 1996, 2:1627-36.
34. Rembrink K, Romijn JC, van der Kwast TH, Rubben H, Schroder FH. Orthotopic implantation of human prostate cancer cell lines: A clinically relevant animal model for metastatic prostate cancer. *Prostate* 1997, 31:168-74.
35. Sato N, Gleave ME, Bruchovsky N, Rennie PS, Beraldi E, Sullivan LD. A metastatic and androgen-sensitive human prostate cancer model using intraprostatic inoculation of Incap cells in SCID mice. *Cancer Res* 1997, 57:1584-9.
36. Thalmann GN, Anezinis PE, Chang SM, Zhau HE, Kim EE, Hopwood VL *et al*. Androgen-independent cancer progression and bone metastasis in the Incap model of human cancer. *Cancer Res* 1994, 54:2577-81.
37. Kusaka N, Nasu Y, Arata R, Saika T, Tsushima T, Kraaij R *et al*. Transrectal ultrasound for monitoring murine orthotopic prostate tumor. *Prostate* 2001, 47:118-24.
38. Meyvisch C. Influence of implantation site on formation of metastasis. *Cancer Metastasis Rev* 1983, 2:295-306.

39. White DC, DeCosse JJ. Experimental arterial dissemination of tumor cells. *Cancer* 1968, 21:9–15.
40. Stackpole CW. Distant lung-colonizing and lung-metastasizing cell populations in B16 mouse melanoma. *Nature* 1981, 289:798–800.
41. Fisher B, Fisher ER. Transmigration of lymph nodes by tumor cells. *Science* 1966, 152:1397–8.
42. Ishibashi T, Yamada H, Harada S, Harada Y, Miyazaki N, Takamoto M, Watanabe K. Distant metastasis facilitated by BCG: Spread of tumor cells injected in the BCG-primed site. *Br J Cancer* 1980, 41:553–61.
43. Kopf-Maier P. Dying and regeneration of human tumor cells after heterotransplantation to athymic mice. *Histol Histopathol* 1986, 1:383–90.
44. Kopf-Maier P, Jackel M. Proliferation behavior of xenografted human tumors: A flow cytometric study. *Anticancer Res* 1988, 8:1355–60.
45. Wilson EL, Gartner M, Campbell JAH, Dowdle EB. Growth and behavior of human melanomas in nude mice. Effect of fibroblasts, pp. 357–61. In: *Immuno-Deficient Animals.*, Sordat B, ed., Karger, 1984.
46. Picard O, Rolland Y, Poupon MF. Fibroblast-dependent tumorigenicity of cells in nude mice: Implication for implantation of metastasis. *Cancer Res* 1986, 46:3290–4.
47. Horgan K, Jones DL, Mansel RE. Mitogenicity of human fibroblasts *in vivo* for human breast cancer cells. *Br J Surg* 1987, 74:227–9.
48. Fridman R, Giaccòne G, Kanemoto T, Martin GR, Gazdar AF, Mulshine JL. Reconstituted basement membrane (matrigel) and laminin can enhance the tumorigenicity and the drug resistance of small cell lung cancer cell lines. *Proc Natl Acad Sci USA* 1990, 87:6689–702.
49. Pretlow TG, Delmoro CM, Dilley GG, Spadafora CG, Pretlow TP. Transplantation of human prostate carcinoma into nude mice in matrigel. *Cancer Res* 1991, 51:3814–7.
50. Fridman R, Kibbey MC, Royce LS, Zain M, Sweeney TM, Jicha DL *et al.* Enhanced tumor growth of both primary and established human and murine tumor cells in athymic mice after coinjection with matrigel. *J Natl Cancer Inst* 1991, 83:769–4.
51. Noel A, Borcy V, Bracke M, Gilles C, Bernard J, Birembaut P *et al.* Heterotransplantation of primary and established human tumor cells in nude mice. *Anticancer Res* 1995, 15:1–8.
52. Kleinman HK. Basement membrane complexes with biological activity. *Biochemistry* 1986, 25:312–8.
53. Liotta LA, Steeg PS, Stetler-Stevenson WG. Metastasis and angiogenesis: An imbalance of positive and negative regulation. *Cancer* 1991, 64:327–6.
54. Passaniti A, Isaacs JT, Haney JA, Adler SW, Cujdik TJ, Long PV, Kleinman HK. Stimulation of human prostate carcinoma tumor growth in athymic mice and control of migration in culture by extracellular matrix. *Int J Cancer* 1992, 51:318–24.
55. Fu X, Besterman JM, Monosov A, Hoffman RM. Models of human metastatic colon cancer in nude mice orthotopically constructed by using histologically-intact patient specimens. *Proc Natl Acad Sci USA* 1991, 88:9345–9.
56. Fu X, Herrera H, Kubota T, Hoffman RM. Extensive liver metastasis from human colon cancer in nude and scid mice after orthotopic onplantation of histologically-intact human colon carcinoma tissue. *Anticancer Res* 1992, 12:1395–8.
57. Fu X, Theodorescu D, Kerbel RS, Hoffman RM. Extensive multi-organ metastasis following orthotopic onplantation of histologically-intact human bladder carcinoma tissue in nude mice. *Int J Cancer* 1991, 49:938–9.

58. Fu X, Hoffman RM. Human RT-4 bladder carcinoma is highly metastatic in nude mice, comparable to rash-transformed RT-4 when orthotopically onplanted as histologically-intact tissue. *Int J Cancer* 1992, 51:989-1.
59. Wang X, Fu X, Hoffman RM. A new patient-like metastatic model of human lung cancer constructed orthotopically with intact tissue via thoracotomy in immunodeficient mice. *Int J Cancer* 1992, 51:992-5.
60. Wang X, Fu X, Hoffman RM. A patient-like metastasizing model of human lung adenocarcinoma constructed via thoracotomy in nude mice. *Anticancer Res* 1992, 12:1399-402.
61. Wang X, Fu X, Kubota T, Hoffman RM. A new patient-like metastatic model of human small-cell lung cancer constructed orthotopically with intact tissue via thoracotomy in nude mice. *Anticancer Res* 1992, 12:1403-6.
62. Kuo T-H, Kubota T, Watanabe M, Furukawa T, Kase S, Tanino H *et al.* Orthotopic reconstitution of human small-cell lung carcinoma after intravenous transplantation in SCID mice. *Anticancer Res* 1992, 12:1407-0.
63. Fu X, Guadagni F, Hoffman RM. A metastatic nude-mouse model of human pancreatic cancer constructed orthotopically from histologically intact patient specimens. *Proc Natl Acad Sci USA* 1992, 89:5645-9.
64. Furukawa T, Fu X, Kubota T, Watanabe M, Kitajima M, Hoffman RM. Nude mouse metastatic models of human stomach cancer constructed using orthotopic implantation of histologically intact tissue. *Cancer Res* 1993, 53:1204-8.
65. An Z, Jiang P, Wang X, Moossa AR, Hoffman RM. Development of a high metastatic orthotopic model of human renal cell carcinoma in nude mice: Benefits of fragment implantation compared to cell-suspension injection. *Clin Exp Metastasis* 1999, 17:265-70.
66. Fu X, Le P, Hoffman RM. A metastatic orthotopic-transplant nude-mouse model of human patient breast cancer. *Anticancer Res* 1993, 13:901-4.
67. Fu X, Hoffman RM. Human ovarian carcinoma metastatic models constructed in nude mice by orthotopic transplantation of histologically-intact patient specimens. *Anticancer Res* 1993, 13:283-6.
68. Chishima T, Miyagi Y, Wang X, Tan Y, Shimada H, Moossa AR, Hoffman RM. Visualization of the metastatic process by green fluorescent protein expression. *Anticancer Res* 1997, 17:2377-84.
69. Chishima T, Miyagi Y, Wang X, Baranov E, Tan Y, Shimada H *et al.* Metastatic patterns of lung cancer visualized live and in process by green fluorescence protein expression. *Clin Exp Metastasis* 1997, 15:547-2.
70. Chishima T, Miyagi Y, Li L, Tan Y, Baranov E, Yang M *et al.* Use of histoculture and green fluorescent protein to visualize tumor cell host interaction. *In Vitro Cell Dev Biol-Animal* 1997, 33:745-7.
71. Chishima T, Yang M, Miyagi Y, Li L, Tan Y, Baranov E *et al.* Governing step of metastasis visualized in vitro. *Proc Natl Acad Sci USA* 1997, 94:11573-6.
72. Yang M, Hasegawa S, Jiang P, Wang X, Tan Y, Chishima T *et al.* Widespread skeletal metastatic potential of human lung cancer revealed by green fluorescent protein expression. *Cancer Res* 1998, 58:4217-21.
73. Dolman CS, Mueller BM, Lode HN, Xiang R, Gillies SD, Reisfeld RA. Suppression of human prostate carcinoma metastases in severe combined immunodeficient mice by interleukin 2 immunocytokine therapy. *Clin Cancer Res* 1998, 4:2551-7.

74. Yang M, Jiang P, Sun FX, Hasegawa S, Baranov E, Chishima T *et al.* A fluorescent orthotopic bone metastasis model of human prostate cancer. *Cancer Res* 1999, 59:781–6.
75. Fidler IJ. Critical factors in the biology of human cancer metastasis: Twenty-eighth G.H.A. clovis memorial award lecture. *Cancer Res* 1990, 50:6130–8.
76. Poste G, Fidler IJ. The pathogenesis of cancer metastasis. *Nature* 1980, 283:139–45.
77. Feldman M, Eisenbach L. What makes a tumor cell metastatic. *Sci Am* 1988, 259(5):60–5, 68, 85.
78. Waters DJ, Janovitz EB, Chan TCK. Spontaneous metastasis of PC-3 cells in athymic mice after implantation in orthotopic or ectopic microenvironments. *Prostate* 1995, 26:227–34.
79. Ozen M, Multani AS, Kuniyasu H, Chung LW, von Eschenbach AC, Pathak S. Specific histologic and cytogenetic evidence for in vivo malignant transformation of murine host cells by three human prostate cancer cell lines. *Oncol Res* 1997, 9(8):433–8.
80. Hall SJ, Thompson TC. Spontaneous but not experimental metastatic activities differentiate primary tumor-derived vs metastasis-derived mouse prostate cancer cell lines. *Clin Exp Metastasis* 1997, 15(6):630–8.
81. Chang XH, Fu YW, Na WL, Wang J, Sun H, Cai L. Improved metastatic animal model of human prostate carcinoma using surgical orthotopic implantation (SOI). *Anticancer Res* 1999, 19(5B):4199–202.
82. Wang X, An Z, Geller J, Hoffman RM. High malignancy orthotopic nude mouse model of human prostate cancer IncaP. *Prostate* 1999, 39:182–6.
83. Mundy GR. Mechanisms of bone metastasis. *Cancer* 1997, 80:1546–56.
84. Maeda H, Segawa T, Kamoto T, Yoshida H, Kakizuka A, Ogawa O, Kakehi Y. Rapid detection of candidate metastatic foci in the orthotopic inoculation model of androgen-sensitive prostate cancer cells introduced with green fluorescent protein. *Prostate* 2000, 45(4):335–40.
85. Patel S, Turner PR, Stubberfield C, Barry E, Rohlf CR, Stamps A *et al.* Hyaluronidase gene profiling and role of hyal-1 overexpression in an orthotopic model of prostate cancer. *Int J Cancer* 2002, 97(4):416–24.
86. Cao G, Su J, Lu W, Zhang F, Zhao G, Marteralli D, Dong Z. Adenovirus-mediated interferon-beta gene therapy suppresses growth and metastasis of human prostate cancer in nude mice. *Cancer Gene Ther* 2001, 8(7):497–505.
87. Chu LW, Pettaway CA, Liang JC. Genetic abnormalities specifically associated with varying metastatic potential of prostate cancer cell lines as detected by comparative genomic hybridization. *Cancer Genet Cytogenet* 2001, 127(2):161–7.
88. Bex A, Wullich B, Endris V, Otto T, Rembrink K, Stockle M, Rubben H. Comparison of the malignant phenotype and genotype of the human androgen-independent cell line DU-145 and a subline derived from metastasis after orthotopic implantation in nude mice. *Cancer Genet Cytogenet* 2001, 124(2):98–104.
89. Timár J, Rásó E, Döme B, Li L, Grignon D, Nie D *et al.* Expression, subcellular localization and putative function of platelet-type 12-lipoxygenase in human prostate cancer cell lines of different metastatic potential. *Int J Cancer* 2000, 87(1):37–43.
90. Inoue K, Slaton JW, Eve BY, Kim SJ, Perrotte P, Balbay MD *et al.* Interleukin 8 expression regulates tumorigenicity, metastases in androgen-independent prostate cancer. *Clin Cancer Res* 2000, 6(5):2104–19.
91. Stearns ME, Wang M. Antimetastatic and antitumor activities of interleukin 10 in transfected human prostate PC-3 ML clones: Orthotopic growth in severe combined

- immunodeficient mice. *Clin Cancer Res* 1998, 4(9):2257-63.
92. Stearns ME, Garcia FU, Fudge K, Rhim J, Wang M. Role of interleukin 10 and transforming growth factor BETA1 in the angiogenesis and metastasis of human prostate primary tumor lines from orthotopic implants in severe combined immunodeficiency mice. *Clin Cancer Res* 1999, 5(3):711-20.
 93. Trikha M, Raso E, Cai Y, Fazakas Z, Paku S, Porter AT *et al.* Role of alpha5(beta1) integrin in prostate cancer metastasis. *Prostate* 1998, 35(3):185-92.
 94. Marengo SR, Sikes RA, Anezinis P, Chang SM, Chung LW. Metastasis induced by overexpression of P185NEU-T after orthotopic injection into a prostatic epithelial cell line (nbe). *Mol Carcinog* 1997, 19(3):165-75.
 95. Greene GF, Kitadai Y, Pettaway CA, von Eschenbach AC, Bucana CD, Fidler IJ. Correlation of metastasis-related gene expression with metastatic potential in human prostate carcinoma cells implanted in nude mice using an in situ messenger RNA hybridization technique. *Am J Pathol* 1997, 150(5):1571-82.
 96. Olson KA, Byers HR, Key ME, Fett JW. Prevention of human prostate tumor metastasis in athymic mice by antisense targeting of human angiogenin. *Clin Cancer Res* 2001, 7(11):3598-605.
 97. Dong Z, Greene G, Pettaway C, Dinney CP, Eue I, Lu W *et al.* Suppression of angiogenesis, tumorigenicity, and metastasis by human prostate cancer cells engineered to produce interferon-beta. *Cancer Res* 1999, 59(4):872-9.
 98. Nasu Y, Bangma CH, Hull GW, Lee HM, Hu J, Wang J *et al.* Adenovirus-mediated interleukin-12 gene therapy for prostate cancer: Suppression of orthotopic tumor growth and pre-established lung metastases in an orthotopic model. *Gene Ther* 1999, 6(3):338-49.
 99. Hull GW, Mccurdy MA, Nasu Y, Bangma CH, Yang G, Shimura S *et al.* Prostate cancer gene therapy: Comparison of adenovirus-mediated expression of interleukin 12 with interleukin 12 plus B7-1 for in situ gene therapy and gene-modified, cell-based vaccines. *Clin Cancer Res* 2000, 6(10):4101-9.
 100. Eastham JA, Grafton W, Martin CM, Williams BJ. Suppression of primary tumor growth and the progression to metastasis with P53 adenovirus in human prostate cancer. *J Urol* 2000, 164(3 Pt 1):814-9.
 101. Hall SJ, Mutchnik SE, Chen SH, Woo SL, Thompson TC. Adenovirus-mediated herpes simplex virus thymidine kinase gene and ganciclovir therapy leads to systemic activity against spontaneous and induced metastasis in an orthotopic mouse model of prostate cancer. *Int J Cancer* 1997, 70(2):183-7.
 102. Hall SJ, Sanford MA, Atkinson G, Chen SH. Induction of potent antitumor natural killer cell activity by herpes simplex virus-thymidine kinase and ganciclovir therapy in an orthotopic mouse model of prostate cancer. *Cancer Res* 1998, 58(15):3221-5.
 103. Maeda H, Hori S, Nishitoh H, Ichijo H, Ogawa O, Kakehi Y, Kakizuka A. Tumor growth inhibition by arsenic trioxide (AS2O3) in the orthotopic metastasis model of androgen-independent prostate cancer. *Cancer Res* 2001, 61(14):5432-40.
 104. Tahir SA, Yang G, Ebara S, Timme TL, Satoh T, Li L *et al.* Secreted caveolin-1 stimulates cell survival/clonal growth and contributes to metastasis in androgen-insensitive prostate cancer. *Cancer Res* 2001, 61(10):3882-5.
 105. Saffran DC, Raitano AB, Hubert RS, Witte ON, Reiter RE, Jakobovits A. Anti-PSCA mAbs inhibit tumor growth and metastasis formation and prolong the survival of mice bearing human prostate cancer xenografts. *Proc Natl Acad Sci U S A* 2001, 98(5):2658-63.

106. Anidjar M, Villette JM, Devauchelle P, Delisle F, Cotard JP, Billotey C *et al.* In vivo model mimicking natural history of dog prostate cancer using DPC-1, a new canine prostate carcinoma cell line. *Prostate* 2001, 46(1):2–10.
107. Yang M, Baranov E, Jiang P, Sun F-X, Li X-M, Li L *et al.* Whole-body optical imaging of green fluorescent protein-expressing tumors and metastases. *Proc Natl Acad Sci USA* 2000, 97:1206–1.
108. Yang M, Baranov E, Li X-M, Wang J-W, Jiang P, Li L *et al.* Whole-ody and intravital optical imaging of angiogenesis in orthotopically implanted tumors. *Proc Natl Acad Sci USA* 2001, 98:2616–1.
109. Yang, Baranov ME, Moossa AR, Penman S, Hoffman RM. Visualizing gene expression by whole-body fluorescence imaging. *Proc Natl Acad Sci USA* 2000, 97:12278–82.
110. Yang M, Baranov E, Wang J-W, Jiang P, Wang X, Sun F-X *et al.* Direct external imaging of nascent cancer, tumor progression, angiogenesis, and metastasis on internal organs in the fluorescent orthotopic model. *Proc Natl Acad Sci USA* 2002, 99:3824–9.
111. Hoffman RM. Orthotopic metastatic mouse models for anticancer drug discovery and evaluation: A bridge to the clinic. *Investigational New Drugs* 1999, 17:343–59.
112. Knox JD, Mack CF, Powell WC, Bowden GT, Nagle RB. Prostate tumor cell invasion: A comparison of orthotopic and ectopic models. *Invasion Metastasis* 1993, 13(6):325–1.
113. Gupta S, Hastek K, Ahmad N, Lewin JS, Mukhtar H. Inhibtion of prostate carcinogenesis in TRAMP mice by oral infusion of green tea polyphenols. *Proc Natl Acad Sci USA* 2001, 98:10350–55.